Available online at www.sciencedirect.com
ScienceDirect
Journal of Power Sources 177 (2008) 537–545
JOURNAL OF POWER SOURCES
www.elsevier.com/locate/jpowsour

# *N*-Methyl-(*n*-butyl)pyrrolidinium bis(trifluoromethanesulfonyl)imide-LiTFSI–poly(ethylene glycol) dimethyl ether mixture as a Li/S cell electrolyte

Joon Ho Shin [a], Elton J. Cairns [a,b,*]

[a] *Environmental Energy Technologies Division, Lawrence Berkeley National Laboratory, One Cyclotron Road, Berkeley, CA 94720, USA*
[b] *Department of Chemical Engineering, University of California, Berkeley, CA 94720, USA*

Received 22 August 2007; received in revised form 12 November 2007; accepted 13 November 2007
Available online 22 November 2007

**Abstract**

We have characterized a ternary mixture of *N*-methyl-(*n*-butyl)pyrrolidinium bis(trifluoromethanesulfonyl)imide ($PYR_{14}TFSI$) + 0.5 M LiTFSI + *y* poly(ethylene glycol) dimethyl ether (PEGDME) (*y* = kg PEGDME/kg $PYR_{14}TFSI$) as an electrolyte in Li metal/S cells. The presence of $PYR_{14}TFSI$ in the mixture resulted in a significant improvement of the thermal stability and the ionic conductivity ($\sigma$) of the mixture with increasing PEGDME contents (for example, $\sigma = 4.2 \times 10^{-3}$ S cm$^{-1}$ at 29 °C for *y* = 2.0). These improvements are most significant at low temperatures, which is probably due to a lowering of the viscosity of the mixture with higher amounts of PEGDME. It is found that the mixture has good compatibility with respect to Li metal as demonstrated by time-dependent interfacial impedance and galvanostatic Li stripping/deposition measurements. We found that a Li/S cell with $PYR_{14}TFSI$ + 0.5 M LiTFSI + *y* PEGDME (*y* = 2.0) can deliver about 1300 mAh g$^{-1}$-sulfur at 0.054 mA cm$^{-2}$ at ambient temperature at the first cycle. A better charge/discharge cyclability of the Li/S cell in $PYR_{14}TFSI$ + 0.5 M LiTFSI + *y* PEGDME was found at higher PEGDME contents, and a Li/S cell with the mixture having *y* = 2.0 exhibited a capacity fading rate of 0.42% per cycle over 100 cycles at 0.054 mA cm$^{-2}$ at 40 °C. Consequently the $PYR_{14}TFSI$ + LiTFSI + PEGDME mixture is a promising electrolyte for Li/S cells.


*Keywords:* Lithium cells; Lithium/sulfur cells; Ionic liquids; Lithium batteries; Lithium electrodes

## 1. Introduction

Li ion batteries are widely being utilized as power sources especially in portable electronics such as mobile phones and laptop computers that require high energy density and long lifetime. However, commercial Li-ion batteries using conventional organic solvents, i.e. ethylene carbonate (EC), diethyl carbonate (DEC) and dimethyl carbonate (DMC), as an electrolyte component still have safety issues due to poor thermal stability leading to decomposition and reaction of these organic solvents at fairly low temperatures (<100 °C). Room temperature ionic liquids (ILs) have been investigated over past decades for possible application as an electrolyte component in batteries [1,2], supercapacitors [3], and polymer light-emitting electrochemical cells [4–6] due to their well-known advantages as follows: high ionic conductivity, non-flammability, wide electrochemical stability window and their environmentally benign nature.

As a formulation of either an IL–Li salt binary mixture [7,8] or an IL–Li salt–organic solvent ternary mixture [9,10] or an IL–Li salt–polymer gel electrolyte [11–13] ILs have been investigated for use in Li batteries as an electrolyte component. We previously found that the incorporation of *N*-methyl-(*n*-alkyl)pyrrolidinium bis(trifluoromethanesulfonyl)imide ($PYR_{1R}TFSI$, the subscript R indicates an alkyl chain) ILs into conventional poly(ethylene oxide) (PEO)-based polymer electrolyte resulted in a significant improvement of ionic conductivity and cycling performance of $Li/V_2O_5$ (or $LiFePO_4$) [14–19].

Sulfur is of great interest as a cathode material since elemental sulfur is able to deliver 1672 mAh g$^{-1}$, assuming that elemental sulfur is fully converted into $Li_2S$. This

* Corresponding author at: Department of Chemical Engineering, University of California, 201 GilmanHall, Berkeley, California 94720, USA.
Tel.: +1 510 486 5028.
*E-mail address:* ejcairns@lbl.gov (E.J. Cairns).

0378-7753/$ – see front matter © 2007 Elsevier B.V. All rights reserved.
doi:10.1016/j.jpowsour.2007.11.043

is the highest theoretical capacity among conventional cathode materials, but it suffers from high-rate capacity fading in combination with normal electrolyte systems, for example PEO-based polymer electrolyte [20] or dioxolane–dimethoxy ethane–diglyme–sulfolane–1 M $LiCF_3SO_3$ mixtures [21]. There were recent reports on the use of ILs as an electrolyte component in a Li/S cell: dimethoxyethane/dioxolane (8/2 v/v)–imidazolium salts (9/1 v/v) ternary mixture [22]; *N*-methyl-(*n*-butyl)piperidinium bis(trifluoromethanesulfonyl)imide–1 M LiTFSI binary mixture [23].

Although there are some reports showing better cycling performance of Li cells in IL–Li salt binary mixtures, in fact such electrolyte systems seem to be faced with an issue of high interfacial impedance at the Li metal electrode, which limits rate capability and long-term cycle life of Li cells. Katayama et al. demonstrated that Li metal in ionic liquid electrolytes forms a protective layer [24], and Howlett et al reported that *N*-methyl-(*n*-alkyl)pyrrolidinium bis(trifluoromethanesulfonyl)amide ionic liquid forms a passive layer on the Li metal surface greater than those with alkyl carbonates that might lead to high interfacial impedance [25]. In a previous work we found that a Li/S cell with poly(ethylene glycol) dimethyl ether (PEGDME) solvent electrolytes is able to deliver above 100 mAh $g^{-1}$-electrode for 600 cycles at room temperature, demonstrating that PEGDME solvent is compatible with Li metal and the intermediates of the sulfur cathode [26]. Therefore, we have employed PEGDME (molecular weight = 250) as a component in the $PYR_{14}TFSI$ IL-LiTFSI-PEGDME mixture in order to improve the compatibility between the electrolyte and Li metal.

In this study, we employ a ternary mixture, $PYR_{14}TFSI + x$ LiTFSI + $y$ PEGDME ($x$ = mols LiTFSI/kg $PYR_{14}TFSI$ and $y$ is the mass ratio of PEGDME/$PYR_{14}TFSI$), as an electrolyte in Li/S cells. We also characterize the physical and electrochemical properties of the mixture as well as the charge and discharge capability of Li/S cells using these mixtures as the electrolyte at various temperatures.

## 2. Experimental equipment and procedures

### 2.1. Materials

*N*-Methyl-(*n*-butyl)pyrrolidinium bis(trifluoromethanesulfonyl)imide ($PYR_{14}TFSI$, see Fig. 1 for chemical structure) ionic liquid salt was synthesized and provided by both Dr. Passerini's group of ENEA and Dr. Henderson of US Naval Academy and dried at about 130 °C overnight in a vacuum oven before use. Elemental sulfur (Sublimed sulfur powder, Alfa Johnson Matthey), carbon black (Shawinigan black, 50% compressed) and poly(vinylidene fluoride) (PVDF, Kynar) were dried in a vacuum oven overnight at 50, 130 and 90 °C, respectively, before use.

### 2.2. Electrolyte preparation

Poly(ethylene glycol) dimethyl ether (PEGDME, Fluka, Molecular weight = 250, chemical structure is presented in Fig. 1) was passed through a column filled with alumina (MP Alumina N-Super I, MP Biomedicals Germany GmbH) to obtain dry polymer with limited $H_2O$ (~30 ppm) level before use. $PYR_{14}TFSI + x$ LiTFSI + $y$ PEGDME mixtures were prepared for which $x$ had value of 0.5 moles per kg of $PYR_{14}TFSI$, and $y$ had values of 0.1, 1.0, 1.5 and 2.0 kg PEGDME per kg of $PYR_{14}TFSI$, and the blend was stirred gently overnight on a magnetic hot-plate at ambient temperature. The electrolyte preparation was carried out in a glove box filled with helium.

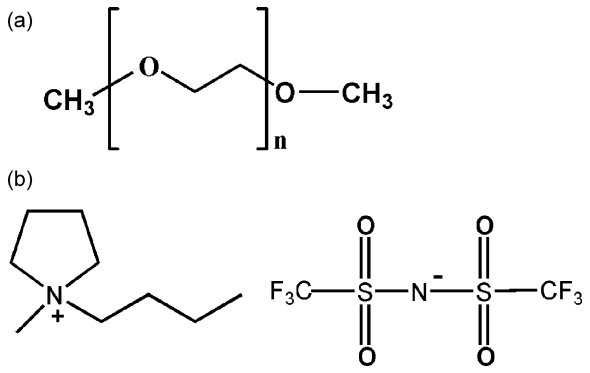


Fig. 1. Chemical structure of poly(ethylene glycol) dimethyl ether (PEGDME) (a) and *N*-methyl-(*n*-butyl)pyrrolidinium ($PYR_{14}^+$) bis(trifluoromethanesulfonyl)imide ($TFSI^-$) (b).

### 2.3. Sulfur cathode preparation

First sulfur powders suspended in ~15 ml of *N*-methylpyrrolidone (dried through a column filled with alumina, NMP, $H_2O$ content of ~30 ppm determined by Karl Fisher Coulometer (Mettler Toledo DL39)) was ball milled for 1 h (referred to as CS1) or 6 h (referred to as CS2) at a rotation speed of 200 rpm using a planetary mono mill (PMM, Pulverisette 6, Fritsch) and then carbon black, PVDF and LiTFSI were added to the ball-milled sulfur suspension and this mixture was ball milled for an additional 1 h (CS1) or 2 h (CS2) under the same conditions. The resulting slurry was coated onto a carbon-coated Al foil substrate using a doctor blade. The solvent was allowed to evaporate overnight at ambient temperature. The resulting cathode film (ca. 50 μm thick) was used to prepare the cathodes by punching circular discs having an area of 0.9 $cm^2$. These discs were dried at ~40 °C under vacuum in the presence of $P_2O_5$ (Aldrich, 97%) for at least 2 days before use. All the procedures for cathode preparation were conducted in a solvent-processing glove box filled with helium. The cathode composition and conditions for planetary milling are presented in Table 1.

### 2.4. Cell assembly and characterization

The thermal behavior and physical properties of $PYR_{14}TFSI + x$ LiTFSI + $y$ PEGDME mixtures were examined using differential scanning calorimetry (DSC, DSC 7, PerkinElmer) over a temperature range of −130 °C to 100 °C with a heating and cooling rate of 10 °C $min^{-1}$ under flow of helium, and thermogravimetric analysis (TGA, TGA 7,

Table 1
Compositions of sulfur cathodes

| | Sulfur (wt.%) | Carbon (wt.%) | PVDF (wt.%) | LiTFSI (wt.%) | $t_{PMM}$ (h) | $D_{sulfur}$ (μm) | Initial discharge capacity (mAh g$^{-1}$-sulfur)[a] | |
|---|---|---|---|---|---|---|---|---|
| | | | | | | | 29(±1) °C | −1(±1) °C |
| CS1[b] | 66.8 | 22.4 | 8.8 | 2.0 | 2 | 28 | 326 | – |
| CS2[c] | 66.7 | 22.4 | 8.9 | 2.0 | 8 | 15 | 1304 | 391 |

$t_{PMM}$ indicates time for planetary mono milling; $D_{sulfur}$ indicates sulfur particle size at 50 v/o determined by particle size analysis after ball milling of the slurry.
[a] The initial discharge capacity was obtained from Li/S cells with $PYR_{14}TFSI$ + 0.5 M LiTFSI + $y$ PEGDME ($y$ = 2.0) electrolyte tested at 0.054 mA cm$^{-2}$.
[b] Sublimed sulfur in CS1 was used as-received.
[c] Sublimed sulfur in CS2 was sieved through 400 mesh (37 μm).

PerkinElmer) was performed at a heating rate of 10 °C min$^{-1}$ from 30 °C to 600 °C under flow of $N_2$.

A symmetric SS/electrolyte/SS cell was used for ionic conductivity measurements, a Li/electrolyte/Li cell was used for interfacial impedance measurements and galvanostatic polarization measurements, and a Li/electrolyte/S cell was used for cell performance and cycling measurements. All of these cells were assembled using a Swagelok cell housing. The separators used were a microporous polypropylene membrane (Celgard 2400) for Li/Li cells and Li/S cells, and a 265 μm thick polypropylene film was used in the SS/SS conductivity cells. The Li metal compatibility with the mixed electrolyte was characterized through AC impedance analysis over a frequency range of from 65 kHz to 0.01 Hz with an amplitude of 5 mV using a Solartron model 1254 in combination with Electrochemical Interface SI1286 and galvanostatic Li stripping/deposition polarization measurements at current density of 0.1–0.2 mA cm$^{-2}$ using a battery cycler (Arbin, BT-2042). The charge and discharge capability of Li/S cells was characterized by galvanostatic charge/discharge over a voltage range of 1.5–3.3 V using the battery cycler. All of the cell preparation and charge/discharge cycling were carried out in a solvent-free glove box filled with helium.

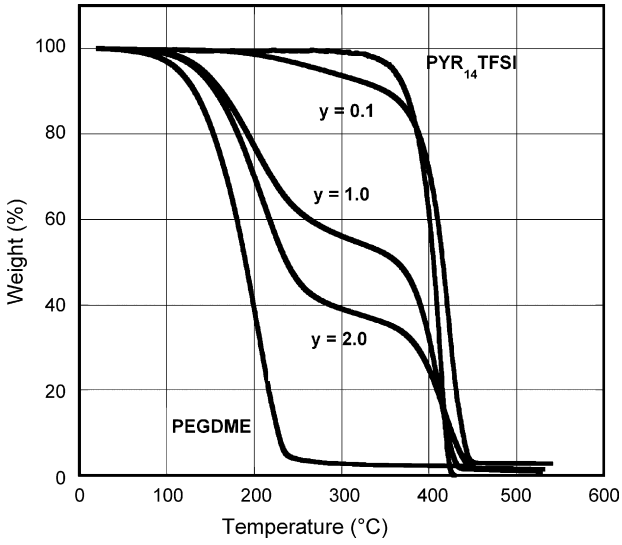


Fig. 2. TGA of $PYR_{14}TFSI$ + 0.5 M LiTFSI + $y$ PEGDME mixture. The measurement was carried out at a heating rate of 10 °C min$^{-1}$ under a $N_2$ atmosphere. The $y$ is the mass ratio of PEGDME-kg/$PYR_{14}TFSI$-kg.

## 3. Results and discussion

The thermal stability of the electrolyte is a crucial issue relating to safety in Li ion batteries. Thermogravimetric analysis was performed on several electrolyte compositions. Fig. 2 shows the weight loss as a function of temperature for $PYR_{14}TFSI$ + 0.5 M LiTFSI + $y$ PEGDME mixtures. The temperatures corresponding to a 5% weight loss for the mixtures are listed in Table 2. Neat ionic liquid $PYR_{14}TFSI$ appeared to be thermally stable up to 300 °C with less than 1% weight loss. A weight loss of 5% was observed at 359 °C that is similar to that (374 °C) for *N*-methyl-(*n*-ethyl)imidazolium TFSI [27]. As reported by Abraham et al. [28] pure PEGDME250 is volatile and exhibited evaporation of some low molecular weight component showing a 1% weight loss at 71 °C and weight loss of 3% at 100 °C. We note that the addition of LiTFSI salt (0.5 mol$^{-1}$kg-PEGDME) to pure PEGDME resulted in somewhat lower weight loss than pure PEGDME under the same conditions and a 3% weight loss of the PEGDME + 0.5 M LiTFSI/kg-PEGMDE mixture was observed at about 107 °C. For $y$ = 0.1 the mixture appeared to

Table 2
Electrochemical and physical properties of $PYR_{14}TFSI$ + 0.5 M LiTFSI + $y$ PEGDME mixtures

| $y$ (kg-PEGDME/kg-$PYR_{14}TFSI$) | $\sigma$ (mS cm$^{-1}$)/T (°C) | $T_g$ (°C) | $T_c$ (°C) | $T_m$ (°C) | [a]$T_{5\%\ weight\ loss}$ (°C) |
|---|---|---|---|---|---|
| 0 | 1.7/30 | −75 | −24 | 7 | 378 |
| 0.1 | 2.9/29 | – | – | – | 276 |
| 1.0 | 3.8/29 | −93 | – | – | 140 |
| 1.5 | 3.5/29 | −105 | −81 | −41 | – |
| 2.0 | 4.2/29 | −104 | −62 | −47 | 135 |
| $PYR_{14}TFSI$[b] | 3.6/30 | −90[b] | −51 | −8 | 359 |
| PEGDME | – | – | – | −35 | 113 |

[a] $T_{5\%\ weight\ loss}$ indicates the temperature resulting 5% weight loss in TGA measurement.
[b] The $T_g$ of $PYR_{14}TFSI$ was attained from the second heating scan at DSC.

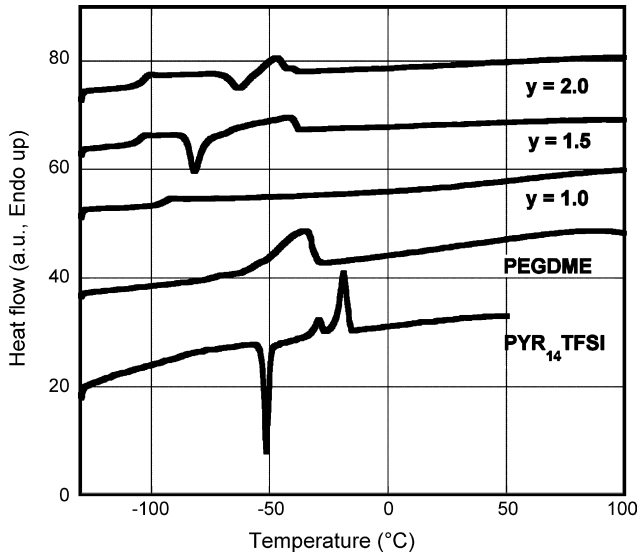


Fig. 3. DSC traces of the first heating scan of $PYR_{14}TFSI + 0.5$ M LiTFSI + $y$ PEGDME mixtures conducted at a scan rate of 10 °C min$^{-1}$ under a helium atmosphere. All the samples were subjected to a second heating scan under the same conditions, but here we only present the first heating scans. The $y$ is the mass ratio of PEGDME-kg/$PYR_{14}TFSI$-kg. First the sample was quenched from room temperature to −130 °C using liquid nitrogen and maintained at −130 °C for about 30 min prior to the start of the measurement. The sample was loaded into an Al pan and sealed hermetically in a glove box filled with He.

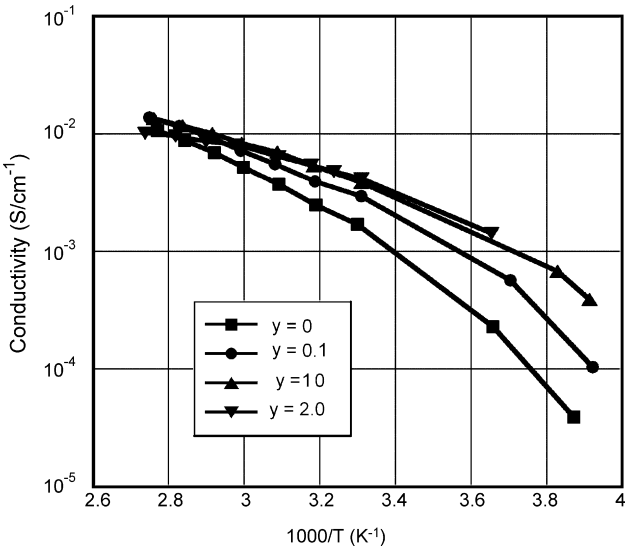


Fig. 4. Arrhenius plot of the ionic conductivity of $PYR_{14}TFSI + 0.5$ M LiTFSI + $y$ PEGDME mixtures. Active area of SS electrode: 0.9 cm$^2$; frequency range: from 65 kHz to 10 Hz. The $y$ is the mass ratio of PEGDME-kg/$PYR_{14}TFSI$-kg. The working temperature was raised from ambient temperature to about 90 °C and all cells were allowed to cool down to ambient temperature overnight in an oven, followed by cooling down to about −15 °C. All cells were equilibrated at every temperature step for at least 30 min prior to AC impedance measurement.

be highly stable with <1.5% weight loss at 200 °C. The mixture with $y = 2.0$ exhibited 1% weight loss at 94 °C and demonstrated relatively good thermal properties. The thermal properties of $PYR_{14}TFSI + 0.5$ M LiTFSI + $y$ PEGDME mixtures are strongly dependent on the amount of PEGDME and lower PEGDME contents in the mixture resulted in better thermal properties of the mixture.

Fig. 3 presents the DSC results for $PYR_{14}TFSI + 0.5$ M LiTFSI + $y$ PEGDME mixtures for the temperature range from −130 °C to 100 °C. The phase transition and glass transition temperatures of the mixtures attained are listed in Table 2. During the first heating scan from −130 °C to 100 °C neat $PYR_{14}TFSI$ ionic liquid exhibited a sharp exothermic peak ($T_{c1}$, phase transition from liquid to phase I) at −51 °C and a metastable phase transition from phase I to phase II at −29 °C ($T_{m1}$) and a melting peak of phase II at −18 °C ($T_{m2}$) which agrees well with the thermal behavior of identical ionic liquid observed by MacFarlane et al. [29] and on the second heating scan the glass transition ($T_g$) at −90 °C and the melting peak of phase II ($T_{m2}$) at −8 °C shifting toward a higher temperature was observed (not shown here). Henderson et al. found a different thermal phase behavior for an identical ionic liquid salt depending upon the thermal history of the sample. Only an endothermic peak at −3 °C was observed as the salt was annealed at −15 °C prior to measurement [30]. For pure PEGDME a broad endothermic peak at −35 °C was found. No phase transition peaks were observed for the mixture with $y = 1.0$. However, both $y = 1.5$ and 2.0 showed an exothermic phase transition at 81 °C and 62 °C, respectively, and for $y = 1.5$ the exothermic peak was not observed on subsequent heating whereas the appearance of the exothermic peak was repeatable in subsequent heating scans for the mixture with $y = 2.0$. We are able to make observations additionally as follows: (i) none of the exothermic ($T_{c1}$) and endothermic peaks ($T_{m1}$ and $T_{m2}$) of neat $PYR_{14}TFSI$ were observed in the DSC trace of $PYR_{14}TFSI + 0.5$ M LiTFSI + $y$ PEGDME mixtures; (ii) an endothermic peak of PEGDME located at −35 °C was only found in the mixtures of higher PEGDME contents above $y = 1.5$, which shifts toward lower temperatures with increasing PEGDME contents; (iii) the glass transition temperature of neat $PYR_{14}TFSI$ positioning at −90 °C was lowered to −105 °C with increasing PEGDME contents in the mixture.

Fig. 4 displays the ionic conductivity of $PYR_{14}TFSI + 0.5$ M LiTFSI + $y$ PEGDME mixtures. The addition of small amounts of PEGDME ($y = 0.1$) to the mixture resulted in a remarkable increase of the ionic conductivity when compared to that of $PYR_{14}TFSI + 0.5$ M LiTFSI ($y = 0$), particularly at low temperatures (<30 °C). The increase of ionic conductivity was apparent with increasing PEGDME contents up to $y = 1.0$ and no substantial increase of ionic conductivity of the mixture with higher PEGDME contents up to $y = 2.0$ was found over entire temperature range studied. The ionic conductivity of $y = 2.0$ was $4.2 \times 10^{-3}$ S cm$^{-1}$ at 29 °C which is comparable to those of organic solvent-based electrolytes, for example diethyl carbonate (DEC) + 40 mol.% propylene carbonate (PC) + LiTFSI (molar ratio of mixed solvent:salt = 20:1) at 30 °C [31]. In particular the mixture showed fairly high ionic conductivity at low temperatures: $1.3 \times 10^{-3}$ S cm$^{-1}$ at 4.6 °C for $y = 1.5$ and $1.4 \times 10^{-3}$ S cm$^{-1}$ at 0.5 °C for $y = 2.0$. We are attributing such a significant increase of ionic conductivity of the mixture to the lowering of viscosity by addition of PEGDME solvent to the $PYR_{14}TFSI + 0.5$ M LiTFSI mixture.

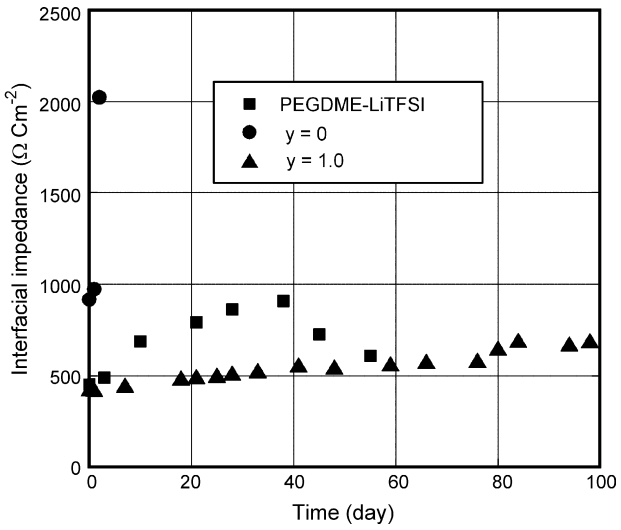


Fig. 5. Interfacial impedance as a function of time for Li/$PYR_{14}TFSI$ + 0.5 M LiTFSI + $y$ PEGDME/Li cells kept at 40 °C under open circuit conditions. The area of the Li electrode was 1.6 cm$^2$. The $y$ is the mass ratio of PEGDME-kg/$PYR_{14}TFSI$-kg. The Li salt concentration in the PEGDME–LiTFSI mixture is 0.5 M LiTFSI/PEGDME-kg.

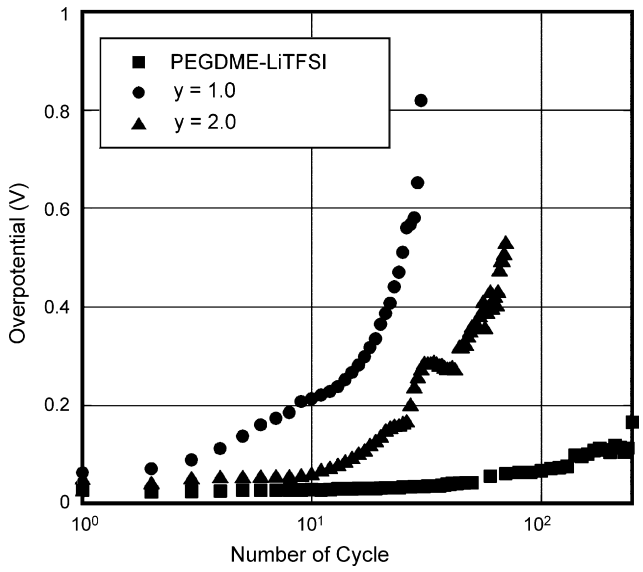


Fig. 6. Anodic overpotential of symmetric Li/$PYR_{14}TFSI$ + 0.5 M LiTFSI + $y$ PEGDME/Li cells acquired from galvanostatic Li stripping/deposition at 0.2 mA cm$^{-2}$ at 60 °C. Area of Li electrode: 1.6 cm$^2$. The $y$ is the mass ratio of PEGDME-kg/$PYR_{14}TFSI$-kg. The PEGDME-LiTFSI mixture contains Li salt of 0.5 M LiTFSI/PEGDME-kg.

Symmetric Li/Li cells in $PYR_{14}TFSI$ + 0.5 M LiTFSI + $y$ PEGDME mixtures were operated at 40 °C under open circuit and the interfacial impedance as a function of time was investigated using an AC impedance analyzer. Fig. 5 shows the behavior of the interfacial impedance of the Li/Li cells with $PYR_{14}TFSI$ + 0.5 M LiTFSI + $y$ PEGDME electrolytes. It is notable that $PYR_{14}TFSI$ + 0.5 M LiTFSI, $y$ = 0, exhibited fairly high interfacial impedance and a steep rise of interfacial impedance was observed within a few days whereas the interfacial impedance of PEGDME + LiTFSI mixtures increased slowly and steadily over about 40 days, followed by a decrease over the following 20 days. The interfacial impedance stabilized over 150 days (not shown in Fig. 5), which demonstrates good compatibility of the PEGDME + LiTFSI mixture with Li metal. The Li/Li cell with the mixture having $y$ = 1.0 showed a steady increase of interfacial impedance over the entire storage time of 109 days with a rate of about 3.6 Ω cm$^2$ day$^{-1}$, and the mixed electrolyte exhibited an excellent compatibility with Li metal at moderate temperatures over three months under open circuit conditions. In conclusion, the presence of PEGDME in the mixture resulted in better compatibility of the mixture toward Li metal and the best compatibility was observed in the presence of both $PYR_{14}TFSI$ and PEGDME.

Fig. 6 displays anodic overpotential versus number of cycles for Li/$PYR_{14}TFSI$ + 0.5 M LiTFSI + $y$ PEGDME/Li cells cycled at 0.334 mA at 60 °C. The cell was held at constant current for 1 h at 0.334 mA and allowed to rest for 1 h followed by passage of current in the opposite direction for 1 h at −0.334 mA, followed by a rest period of 1 h. As shown in Fig. 7, a symmetric overpotential behavior was observed. It is notable that a Li/Li cell in $PYR_{14}TFSI$ + 0.5 M LiTFSI ($y$ = 0) electrolyte showed a drastic increase of overpotential (reached more than 1.5 V within an hour) at 0.334 mA at 60 °C which may be attributed to a fast-growing interfacial impedance for the $PYR_{14}TFSI$ + 0.5 M LiTFSI electrolyte in contact with Li metal as demonstrated by the impedance analysis discussed above (see also Fig. 5) whereas the Li/Li cell with the PEGDME + LiTFSI mixture exhibited relatively low overpotential (<0.2 V) at 0.334 mA at 60 °C for more than 260 cycles. The PEGDME + LiTFSI mixture resulted in the best Li stripping/deposition cycling performance, and the Li/Li cell in $PYR_{14}TFSI$ + 0.5 M LiTFSI + $y$ PEGDME electrolytes showed a lower overpotential and better cycling performance with increasing PEGDME contents up to $y$ = 2.0.

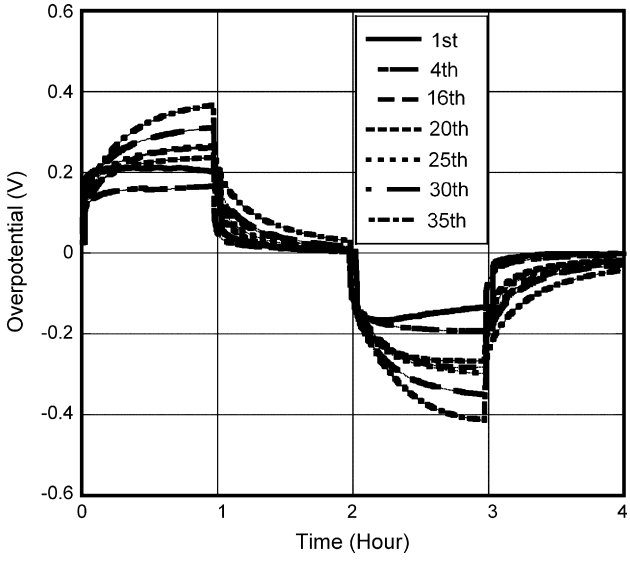


Fig. 7. Selected overpotential profiles of a symmetric Li/$PYR_{14}TFSI$ + 0.5 M LiTFSI + $y$ PEGDME ($y$ = 1.5)/Li cell during galvanostatic Li stripping/deposition at ±0.1 mA cm$^{-2}$ at different temperatures: 30 °C (from the 1st to 15th cycle); 40 °C (from the 16th to 45th cycle). Area of Li electrode: 1.6 cm$^2$. The $y$ is the mass ratio of PEGDME-kg/$PYR_{14}TFSI$-kg.

Fig. 7 presents overpotential profiles of a Li/Li cell with $PYR_{14}TFSI + 0.5$ M LiTFSI + $y$ PEGDME ($y = 1.5$) carried out at 0.167 mA at different temperatures. It is apparent that the Li stripping and deposition profile is symmetric and both polarization profiles showed a rapid increase of overpotential immediately after applying the current and reached a constant level of overpotential. The total overpotentials increased up to ±0.4 V over 35 cycles, which is attributed to the increasing interfacial impedance of the cell as demonstrated by AC impedance analysis (not shown here). The time to reach a steady-state overpotential on cycling appeared to become longer with increasing numbers of cycles, and during the rest periods the relaxation of the concentration gradient formed during current flow takes place more slowly with increasing numbers of cycles. This may be the result of increasing viscosity of the electrolyte with continuing cycling, or an increase of thickness of a SEI formed on the Li.

We investigated the behavior of these electrolyte mixtures in Li/S cells. We used two kinds of sulfur cathodes (referred to as CS1 and CS2) composed of nearly identical compositions only having different sulfur particle sizes as reported in Table 1. The sulfur cathode CS1 with the larger sulfur particle size exhibited a lower initial capacity than CS2 with smaller particle size. Note that the $PYR_{14}TFSI + 0.5$ M LiTFSI + $y$ PEGDME mixture has no phase separation, and neither the sulfur cathode nor separator has wetting issues (that are apparent with the IL alone) with the mixture.

As indicated in Table 1, a Li/S cell with $PYR_{14}TFSI + 0.5$ M LiTFSI + $y$ PEGDME ($y = 2.0$) can deliver about 1300 mAh $g^{-1}$-sulfur at 0.054 mA $cm^{-2}$ at ambient temperature on the first cycle, suggesting that the discharge product of the elemental S reduction reaction is $Li_2S$. The first recharge also shows a specific capacity near 1300 mAh $g^{-1}$ S. This specific capacity of more than 825 mAh $g^{-1}$ S rules out the possibility that $Li_2S_2$ is the final discharge product. Rauh et al. studied the characteristics of Li/dissolved sulfur as $Li_2S_n$ in hydrofuran (THF) solvent and reported that the solubility of $Li_2S_n$ is a crucial factor achieving high utilization of active material. [32]. It is therefore likely that the lithium polysulfides have some solubility in the electrolyte.

Fig. 8 exhibits the charge/discharge behavior of Li/S cells with $PYR_{14}TFSI + 0.5$ M LiTFSI + $y$ PEGDME electrolytes tested at 0.054 mA $cm^{-2}$ at 40 °C. The Li/S cell with $PYR_{14}TFSI + 0.5$ M LiTFSI ($y = 0$) electrolyte exhibited a very low discharge capacity, corresponding to sulfur utilization (= delivered capacity × 100/theoretical capacity of sulfur) of 8.1%, for the first cycle as compared to $PYR_{14}TFSI + 0.5$ M LiTFSI + $y$ PEGDME mixture electrolyte and a relatively high rate capacity fading of 1.62% per cycle, defined as (capacity at 1st cycle − capacity at last cycle) × 100/number of cycle, over 50 cycles was observed, which is higher than those of Li/S cell with $PYR_{14}TFSI + 0.5$ M LiTFSI + $y$ PEGDME mixture, showing capacity fading rate of 1.31, 0.69 and 0.42% per cycle for $y = 1.0$, 1.5 and 2.0, respectively. The cell with $y = 1.0$ showed higher initial discharge capacity than those of the cells with $y = 1.5$ and 2.0, but a rapid capacity fading was observed in the subsequent few cycles, followed by an increase of discharge capacity up to 20 cycles and a large decay of capacity was found over the 80 cycles. The cells with $y = 1.5$ and 2.0 exhibited a similar trend of capacity with a lower rate of capacity fade depending upon the PEGDME contents mentioned above. It is apparent that the cell with $y = 2.0$ showed very reversible charge/discharge behavior from the 60th cycle to the 100th cycle at which point the cell was able to deliver about 269 mAh $g^{-1}$-sulfur (179 mAh $g^{-1}$-electrode), corresponding to about 16% of the theoretical capacity. Consequently, Li/S cells with ternary mixtures of $PYR_{14}TFSI + 0.5$ M LiTFSI + $y$ PEGDME electrolyte containing higher PEGDME contents demonstrated a better charge/discharge cyclability at moderate temperature.

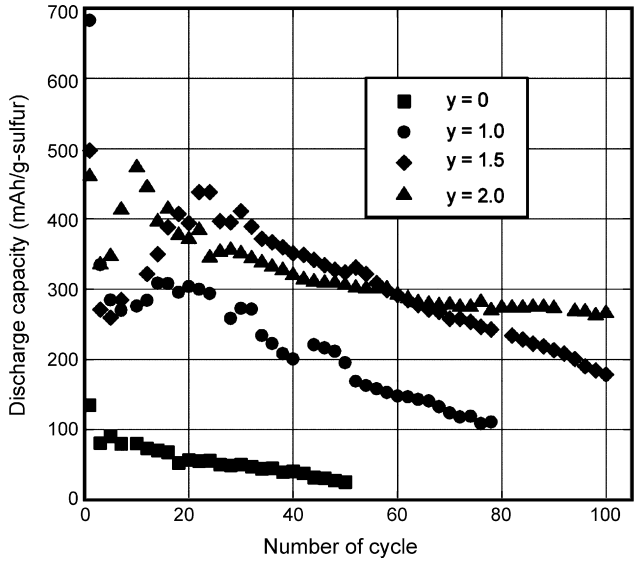


Fig. 8. Discharge capacities of Li/S cells with $PYR_{14}TFSI + 0.5$ M LiTFSI + $y$ PEGDME electrolytes cycled at ±0.054 mA $cm^{-2}$ at 40 °C. The $y$ is a mass ratio of PEGDME-kg/$PYR_{14}TFSI$-kg. Sulfur cathode composition: CS1 (see Table 1); active area of electrodes: sulfur cathode (0.9 $cm^2$), Li anode (1.6 $cm^2$); loading of active material: 2.6 mg ($y = 0$), 0.8 mg ($y = 1.0$), 1.1 mg ($y = 1.5$), 1.3 mg ($y = 2.0$); cut-off voltages: $1.5 < V < 3.3$. All cells were cycled in a glove box filled with He.

After the 100th cycle of the cell with $y = 1.5$ presented in Fig. 8 the sulfur cathode was removed from the cell and reassembled with a fresh Li anode, separator and the electrolyte of $y = 1.5$, and then tested under identical conditions at 0.054 mA $cm^{-2}$ at 40 °C. It is of interest to note that the cell delivered about 720 mAh $g^{-1}$-sulfur for the first discharge that is higher than the initial discharge capacity (498 mAh $g^{-1}$-sulfur) of as assembled cell shown in Fig. 8 and exhibited a good reversible cyclability up to 10 additional cycles showing 723 mAh $g^{-1}$-sulfur at the tenth discharge. In subsequent cycles the current density was varied and Fig. 9 shows a few selected charge/discharge profiles of the reassembled Li/$PYR_{14}TFSI + 0.5$ M LiTFSI + $y$ PEGDME ($y = 1.5$)/S cell carried out at current densities of 0.033, 0.054, 0.11 mA $cm^{-2}$ at 40 °C. Note that the original cell shown in Fig. 8 exhibited a very short discharge plateau at 2.0 V. However, the reassembled cell in Fig. 9 showed a prolonged charge and discharge plateau at 2.0 V (referred to as the lower plateau) and 2.4 V (referred to as the upper plateau), respectively. The cell delivered about 300 mAh $g^{-1}$-sulfur for the upper discharge plateau independent of current density whereas the discharge capacity of the lower plateau appeared to be dependent on cur-

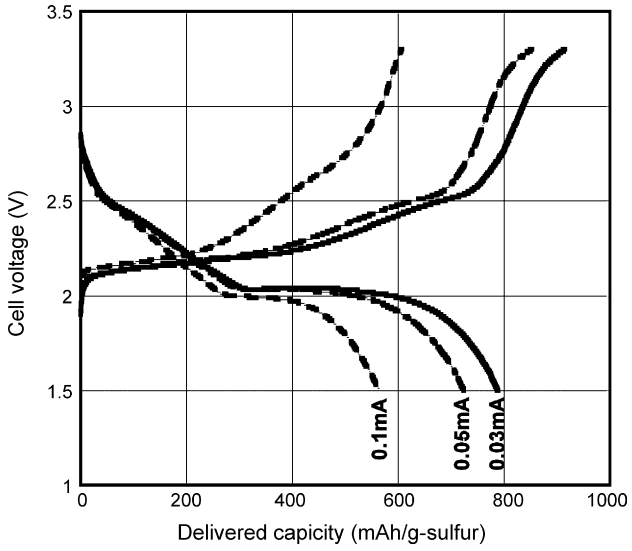


Fig. 9. Voltage profiles of a Li/S cell with $PYR_{14}TFSI + 0.5\,M$ LiTFSI + $y$ PEGDME ($y = 1.5$) electrolyte cycled at 0.054 mA $cm^{-2}$ at 40 °C. The cell with $y = 1.5$ of Fig. 8 was reassembled after 100 cycles using a fresh Li metal electrode and electrolyte ($y = 1.5$). The $y$ is the mass ratio of PEGDME-kg/$PYR_{14}TFSI$-kg. Sulfur cathode composition: CS1 (see Table 1); active area of electrodes: sulfur cathode (0.9 $cm^2$), Li anode (1.6 $cm^2$); loading of active material: 1.1 mg; cut-off voltage: $1.5 < V < 3.3$. The cell was cycled in a glove box filled with He.

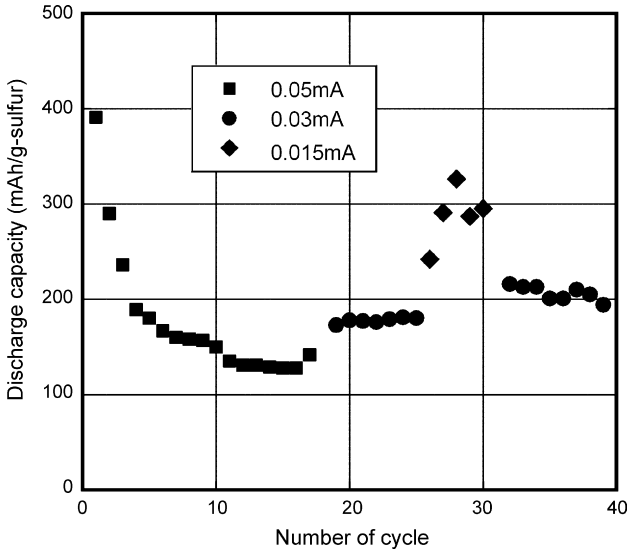


Fig. 10. Discharge capacity vs. number of cycle of Li/$PYR_{14}TFSI + 0.5\,M$ LiTFSI + $y$ PEGDME ($y = 2.0$)/S cell tested at various currents as indicated in the inset at −1.0 °C. The $y$ is a mass ratio of PEGDME-kg/$PYR_{14}TFSI$-kg. Sulfur cathode composition: CS2 (see Table 1); active area of electrodes: sulfur cathode (0.9 $cm^2$), Li anode (1.6 $cm^2$); loading of active material: 1.6 mg; cut-off voltage: $1.5 < V < 3.3$. The cell was kept overnight at working temperature (−1.0 °C) under open circuit prior to cycling.

rent density. The lower current densities resulted in longer lower plateaus, demonstrating that lithium sulfide ($Li_2S$) is more effectively formed at low current densities at moderate temperatures. It is of great importance to point out that the sulfur cathode maintains its active material (elemental sulfur) over long-term cycling indicating that intermediate polysulfides are compatible with these ternary mixtures $PYR_{14}TFSI$-LiTFSI-PEGDME and that capacity fading of the Li/S cell may be correlated with the mechanical degradation of the sulfur cathode such as either poor electric contact between sulfur particles and carbon particles or agglomeration of carbon nano-particles rather than loss of polysulfide or lithium sulfide into the electrolyte.

The low temperature cyclability of Li/S cells in $PYR_{14}TFSI + 0.5\,M$ LiTFSI + $y$ PEGDME ($y = 2.0$) is presented in Fig. 10. The cell was able to deliver about 400 mAh $g^{-1}$-sulfur at −1.0 °C for the first discharge, followed by a rapid capacity decay in a few cycles, and in subsequent cycles the cell exhibited a constant capacity behavior. The initial discharge capacity of the cell at a high current density of 0.054 mA $cm^{-2}$, corresponding to 31.3 mA $g^{-1}$-sulfur, appeared to be comparable to the first discharge capability (approximately 900 mAh $g^{-1}$-sulfur) of a Li/S cell with tetra ethylene glycol dimethyl ether electrolyte containing 0.5 M LiTFSI measured at 0 °C at low specific current of 10 mA $g^{-1}$-sulfur [33] since the cell in Fig. 10 was tested at three times higher current than that of Ref. [33]. The discharge capacity increased accordingly as current density decreased and was apparently constant at each current density. The cell exhibited a constant capacity of about 130 (at the 16th cycle), 180 (at the 25th cycle) and 295 mAh $g^{-1}$-sulfur (at the 30th cycle) at 0.05, 0.03 and 0.015 mA, respectively, and we found that in subsequent cycles the cell showed a better discharge capability compared to those observed in previous cycles at 0.03 mA. The influence of current density on charge and discharge behavior is shown in Fig. 11. At 0.03 mA the upper plateau was definitely prolonged compared to that at 0.05 mA and a remarkable extension of the lower discharge plateau was found at 0.015 mA. These results may imply that lithium polysulfide formation ($Li_2S_n$, $n = 8$) is more efficient at low current density (∼0.0112 C) at low temperature, and

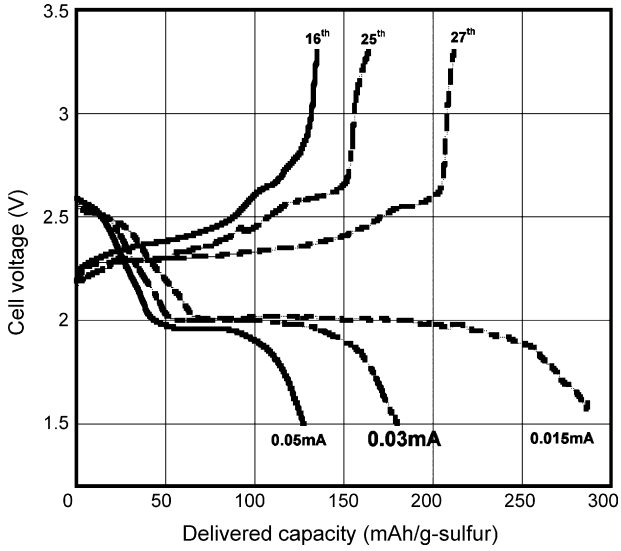


Fig. 11. Selected voltage profiles of Li/$PYR_{14}TFSI + 0.5\,M$ LiTFSI + $y$ PEGDME ($y = 2.0$)/S cell conducted at various currents at −1.0 °C presented in Fig. 10: 0.05 mA (31.3 mA $g^{-1}$-sulfur), 0.03 mA (18.8 mA $g^{-1}$-sulfur) and 0.015 mA (9.4 mA $g^{-1}$-sulfur). The $y$ is a mass ratio of PEGDME-kg/$PYR_{14}TFSI$-kg. Sulfur cathode composition: CS2 (see Table 1); active area of electrodes: sulfur cathode (0.9 $cm^2$), Li anode (1.6 $cm^2$); loading of active material: 1.6 mg; cut-off voltage: $1.5 < V < 3.3$.

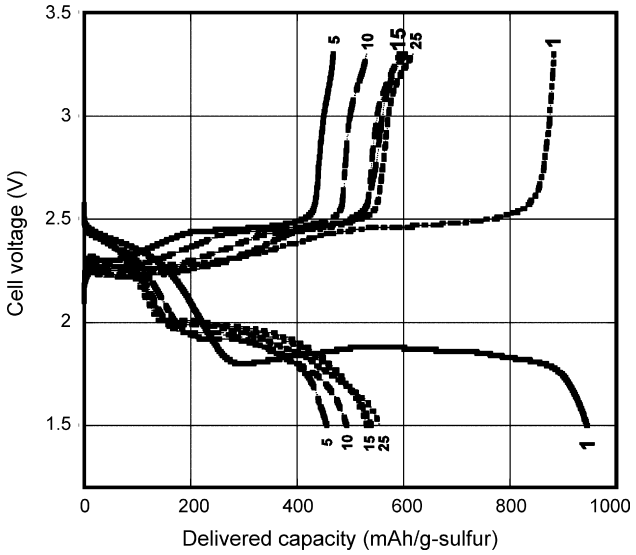


Fig. 12. Selected voltage profiles of Li/$PYR_{14}TFSI$ + 1.5 M LiTFSI + $y$ PEGDME ($y$ = 2.0)/S cell measured at 0.05 mA $cm^{-2}$ at room temperature. The $y$ is the mass ratio of PEGDME-kg/$PYR_{14}TFSI$-kg. Sulfur cathode composition: CS2 (see Table 1); active area of electrodes: sulfur cathode (0.9 $cm^2$), Li anode (1.6 $cm^2$); loading of active material: 1.3 mg; cut-off voltage: $1.5 < V < 3.3$. The cell was cycled in a glove box filled with He.

lithium sulfide is effectively formed at a very slow discharge rate (C/180). An interesting observation is therefore that the rate of formation of lithium polysulfide and lithium sulfide in Li/S cells strongly affected by operating temperature.

The charge and discharge profiles of a Li/S cell with $PYR_{14}TFSI$ + 1.5 M LiTFSI + $y$ PEGDME ($y$ = 2.0) electrolyte tested at 0.054 mA $cm^{-2}$ at room temperature are presented in Fig. 12. The first discharge profile showed a lower discharge plateau in the vicinity of 1.8 V that is somewhat lower than the 2.0 V of a typical lower discharge plateau (see Figs. 9 and 11) for different electrolytes (for example PEO- [34] or PVDF-based electrolyte [35]), which may be attributed to the higher Li salt concentration leading to a higher viscosity of the electrolyte. The lower plateau was observed at about 2 V in following cycles. It is of interest that the cell was able to deliver 945 mAh $g^{-1}$-sulfur (i.e. 56.6% of the theoretical capacity) for the first discharge which is higher than the 45% utilization of a sulfur cell with PEGDME + LiTFSI electrolyte measured at 0.05 mA $cm^{-2}$ at room temperature [36]. At the second cycle a rapid capacity decay occurred, but the capacity increased steadily in subsequent cycles up to 20 cycles, followed by a constant discharge capacity behavior up to 25cycles.

## 4. Conclusions

We have prepared electrolytes as a mixture of $PYR_{14}TFSI$ + 0.5 M LiTFSI + $y$ PEGDME ($y$ = PEGDME-kg/$PYR_{14}TFSI$-kg) with various PEGDME contents from $y$ = 0.1 to 2.0, have characterized them, and employed them in Li/S cells. The presence of $PYR_{14}TFSI$ in the mixture resulted in a significant improvement of thermal stability and ionic conductivity. The ionic conductivity of the mixture increased remarkably with increasing PEGDME contents (for example, for $y$ = 2.0, $\sigma = 4.2 \times 10^{-3}$ S $cm^{-1}$ at 29 °C). The conductivity increase is particularly significant at low temperatures, and is probably due to a lowering of the viscosity of the mixture with higher amounts of PEGDME. It is found that the mixture has good compatibility with Li metal electrodes as demonstrated by time-dependent interfacial impedance and galvanostatic Li stripping/deposition measurements. We found that Li/S cells in $PYR_{14}TFSI$ + 0.5 M LiTFSI + $y$ PEGDME ($y$ = 2.0) can deliver about 1300 mAh $g^{-1}$-sulfur at 0.054 mA $cm^{-2}$ at ambient temperature on the first cycle. A better charge/discharge cyclability of Li/S cells with $PYR_{14}TFSI$ + 0.5 M LiTFSI + $y$ PEGDME was found at higher PEGDME contents, and the Li/S cell with the mixture having $y$ = 2.0 exhibited a capacity fading rate of 0.42% per cycle for over 100 cycles at 0.054 mA $cm^{-2}$ at 40 °C. The $PYR_{14}TFSI$ + LiTFSI + PEGDME mixtures appear to be appropriate electrolytes for Li/S cells.

## Acknowledgements

This work was supported by the Director, Office of Basic Energy Sciences, Chemical Sciences Division of the U.S. Department of Energy, under Contract DE-AC03-76SF00098. The authors thank Dr. Stefano Passerini of ENEA for kindly providing the ionic liquid samples and Dr. John Kerr of LBNL for helpful discussion. We express our great appreciation to Dr. Wesley Henderson of the U.S. Naval Academy for the samples of the ionic liquids used in this work.

## References

[1] Y.S. Fung, S.M. Chau, J. Appl. Electrochem. 23 (1993) 346.
[2] D.R. MacFarlane, J. Huang, M. Forsyth, Nature 402 (1999) 792.
[3] A. Balducci, R. Dugas, P.L. Taberna, P. Simon, D. Plee, M. Mastragostino, S. Passerini, J. Power Sources 165 (2007) 922.
[4] S. Panozzo, M. Armand, O. Stephan, Appl. Phys. Lett. 80 (2002) 679.
[5] J.-H. Shin, S. Xiao, A. Fransson, L. Edman, Appl. Phys. Lett. 87 (2005) 043506.
[6] J.-H. Shin, L. Edman, J. Am. Chem. Soc. 128 (2006) 155568.
[7] H. Sakaebe, H. Matsumoto, Electrochem. Commun. 5 (2003) 594.
[8] S. Seki, Y. Kobayashi, H. Miyashiro, Y. Ohno, A. Usami, Y. Mita, M. Watanabe, N. Terada, Chem. Commun. 5 (2006) 544.
[9] T. Sato, T. Maruo, S. Marukane, K. Takagi, J. Power Sources 138 (2004) 253.
[10] A. Chagnes, M. Diaw, P. Willmann, D. Lemordant, J. Power Sources 145 (2005) 82.
[11] B. Singh, S.S. Sekhon, J. Phys. Chem. B 109 (2005) 16539.
[12] T. Sato, S. Marukane, T. Narutomi, T. Akao, J. Power Sources 164 (2007) 390.
[13] M.A. Klingshirn, S.K. Spear, R. Subramanian, J.D. Holbrey, J.G. Huddleston, R.D. Rogers, Chem. Mater. 16 (2004) 3091.
[14] J.-H. Shin, W.A. Henderson, S. Passerini, Electrochem. Commun. 5 (2003) 1016.
[15] J.-H. Shin, W.A. Henderson, S. Passerini, Electrochem, Solid State Lett. 8 (2005) A125.
[16] J.-H. Shin, W.A. Henderson, S. Passerini, J. Electrochem. Soc. 152 (2005) A978.
[17] J.-H. Shin, W.A. Henderson, S. Scaccia, P. Prosini, S. Passerini, J. Power Sources 156 (2006) 560.
[18] J.-H. Shin, W.A. Henderson, C. Tizzani, S. Passerini, S.-S. Jeong, K.-W. Kim, J. Electrochem. Soc. 153 (2006) A1649.
[19] J.-H. Shin, W.A. Henderson, G.B. Appetecchi, S. Passerini, Electrochem. Acta 50 (2005) 3859.

[20] J.-H. Shin, K.W. Kim, H.J. Ahn, J.H. Ahn, Mater. Sci. Eng. B 95 (2002) 148.
[21] S.-E. Cheon, S.-S. Choi, J.-S. Han, Y.-S. Choi, B.-H. Jung, H.S. Lim, J. Electrochem. Soc. 151 (2004) A2067.
[22] S. Kim, Y. Jung, S.-J. Park, J. Power Sources 52 (2007) 2116.
[23] L.X. Yuan, J.K. Feng, X.P. Ai, Y.L. Cao, S.L. Chen, H.X. Yang, Electrochem. Commun. 8 (2006) 610.
[24] Y. Katayama, T. Morita, M. Yamagata, T. Miura, Electrochemistry (Tokyo, Jpn.) 71 (2003) 1033.
[25] P.C. Howlett, N. Brack, A.F. Hollenkamp, M. Forsyth, D.R. MacFarlane, J. Electrochem. Soc. 153 (2006) A595.
[26] J. Shim, K.A. Striebel, E.J. Cairns, J. Electrochem. Soc. 149 (2002) A1321.
[27] M. Ishikawa, T. Sugimoto, M. Kikuta, E. Ishiko, M. Kono, J. Power Sources 162 (2006) 658.
[28] K.M. Abraham, Z. Jiang, B. Carroll, Chem. Mater. 9 (1997) 1978.
[29] D.R. MacFarlane, P. Meakin, N. Amini, M. Forsyth, J. Phys. Condens. Matter 13 (2001) 8257.
[30] W.A. Henderson, S. Passerini, Chem. Mater. 16 (2004) 2881.
[31] K. Hayamizu, Y. Aihara, Electrochim. Acta 49 (2004) 3397.
[32] R.D. Rauh, K.M. Abraham, G.F. Pearson, J.K. Surprenant, S.B. Brummer, J. Electrochem. Soc. 126 (1979) 523.
[33] H.-S. Ryu, H.-J. Ahn, K.-W. Kim, J.-H. Ahn, K.-K. Cho, T.-H. Nam, J.-U. Kim, G.-B. Cho, J. Power Sources 163 (2006) 201.
[34] J.-H. Shin, Y.-T. Lim, K.-W. Kim, H.-J. Ahn, J.-H. Ahn, J. Power Sources 107 (2002) 103.
[35] H.S. Ryu, H.J. Ahn, K.W. Kim, J.H. Ahn, J.Y. Lee, E.J. Cairns, J. Power Sources 140 (2005) 365.
[36] D. Marmorstein, T.H. Yu, K.A. Striebel, F.R. McLarnon, J. Hou, E.J. Cairns, J. Power Sources 89 (2000) 219.